

## **Numerical investigation of free surface flood wave and solitary wave using incompressible SPH method**

Mohammad Zounemat-Kermani<sup>1</sup>  
Habibeh Sheybanifard<sup>2</sup>

### **Abstract**

Simulation of free surface flow and sudden wave profile are recognized as the most challenging problem in computational hydraulics. Several Eulerian/Lagrangian approaches and models can be implemented for simulating such phenomena in which the smoothed particle hydrodynamics method (SPH) is categorized as a proper candidate. The incompressible SPH (ISPH) method hires a precise incompressible hydrodynamic formulation to calculate the pressure of fluid, and the numerical solution is obtained by using a two-step semi-implicit scheme. This study presents an ISPH method to simulate three free surface problems; (1) a problem of sudden dam-break flood wave on a dry bed with and obstacle in the downstream, (2) a test case of the gradual collapse of the water column on a wet bed and (3) a case of solitary wave propagation problem. The model has been confirmed based on the results of experiments for the dam-break problems (in which was set up by the authors) as well as the collapse of the water column test case and analytical calculations for the solitary wave simulation. The computational results with a mean relative error less than 10%/4% for the wave height/wave front position, demonstrated that the applied ISPH flow model is an appropriate modeling tool in free surface hydrodynamic applications.

**Keywords:** Free-surface flows, Dam-break, Solitary wave, Incompressible smoothed particle hydrodynamics

Received: 04 October 2016; Accepted: 17 November 2016

### **1. Introduction**

Free surface flows and currents are accompanied with deformation and fragmentation of the free surface and solid boundaries. These fragmentations and Deformations in dealing with massive flows of dam-break are exacerbated. There are two major approaches of Eulerian and Lagrangian techniques for modeling of free surface flows. However, most of numerical modeling and studies of fluid flow are mainly based on the Eulerian mesh based formulations such as finite difference, finite-volume and finite-element methods.

Although the ability of these approaches for a wide range of numerical problems have been proven, but these models might be limited for complicated phenomena with large fragmentations and deformations due to their mesh adaptability and connectivity restrictions [1]. In recent years, Lagrangian numerical models have been further developed and their usage is becoming increasingly attractive.

---

<sup>1</sup>Associate professor, Water Engineering Department, Shahid Bahonar University of Kerman, Kerman, Iran, Email: zounemat@uk.ac.ir (**Corresponding author**)

<sup>2</sup> M.Sc of water structures, Water Engineering Department, Shahid Bahonar University of Kerman, Kerman, Iran, 0913939928, Email: habibeh.sheybani@gmail.com

In a Lagrangian method, advection term is calculated by direct movement of particles. Therefore, there is no numerical diffusion [12]. The SPH numerical models, which enable the simulation of complicated and complex free surface flows, are considered as a purely Lagrangian approach [11]. The SPH was developed by Lucy, Gingold and Monaghan (1977) in astrophysics to perusal the impact of stars and galaxies and bolides on planets [16].

Recently, incompressible SPH (ISPH) and weakly compressible SPH (WCSPH) methods (due to their flexibility and power as numerical methods) have been applied to a whole of fluid flow problems (such as the study of gravity currents [4], wave propagation [2], wave interaction on the coastal and offshore structures [8]; [7]) and dam-break flow [15], [6], [7], [17] and [13]). In this respect, Monaghan (1999) used weak compressible SPH Approach for modeling solitary wave along the offshore [12].

Colagrossi and Landrini (2003) implemented SPH method to treat two-dimensional interfacial flows with different fluids separated by sharp interfaces [2]. Ataie-Ashtiani and Shobeyri (2008) presented an incompressible-smoothed particle hydrodynamics (ISPH) formulation to simulate impulsive waves generated by landslides [4]. The results proved the efficiency and applicability of the ISPH approach for simulation of these kinds of complex free surface problems.

Shao (2010) investigated wave interplay with porous media by ISPH procedure [21]. Zhu (2009) used ISPH technique for investigating wave interaction by porous media. Lind et al (2012) introduced a generalized algorithm for validations and stability of propagating waves as well as impulsive flow [18]. Džebo et al (2014) described two different ways of defining the terrain roughness in SPH simulations performed for simulating dam-break phenomenon at the storage reservoir of a hydropower plant in Slovenia [7].

Lind et al (2015) presented a new incompressible-compressible (water-air) smoothed particle hydrodynamics method to model wave slam [19]. Altomare et al (2015) applied the validation of an SPH-based technique for wave loading and strike on coastal structures [6]. Altomare et al (2015) used the SPH-based technique for examination of the interaction for wave and coastal structures. Such as vertical structures and storm return walls [6].

Jonnsson et al (2015) modeled dam-break phenomenon on a wet bed with SPH method. In this paper, the ISPH method has been used for modeling free surface flow. As presented by [20], in the ISPH numerical method, the governing equations of continuity and momentum are solved in a two-step projection method. In the ISPH, the pressure term is implicitly resulted by solving the Poisson equation in the second projection step.

As a result, pressure fluctuation would be less in the ISPH than in comparison with the WCSPH method (where slight compressibility is applied via the equation of state) [20]. In this respect, three test cases of 1) dam-break flow over dry bed and encountering an obstacle, 2) gradual collapsing of the water column over a wet bed, and 3) a solitary wave were modelled in this research using ISPH model.

The accuracy of the ISPH model to simulate flood waves and solitary wave flows is assessed with contrasting the calculated results with those measured by experimental observations and analytical calculation. The governing equation of motion, ISPH formulation, solving algorithm and results of the advanced model are shown in the following sections.

## 2. Governing equations of flow and discretization

Governing equations of wave flow are just mass conservation equations and momentum conservation as follows:

$$\frac{1}{\rho} \frac{D\rho}{Dt} + \nabla \cdot u = 0 \quad (1)$$

$$\frac{Du}{Dt} = -\frac{1}{\rho} \nabla p + \frac{\mu}{\rho} \nabla^2 u + fb \quad (2)$$

where  $\rho$  is density,  $u$  is velocity vector,  $P$  is pressure, and  $fb$  is an external force. Discretization of pressure terms and viscosity in Navier-Stokes (NS) equations by smoothed particle hydrodynamics method is like below:

$$\frac{1}{\rho_i} (\nabla p_i) = \sum_j m_j \left( \frac{p_j}{\rho_j^2} \right) \nabla_i \hat{w}_{ij} + \left( \frac{p_i}{\rho_i^2} \right) \sum_j m_j \cdot \nabla_i \hat{w}_{ij} \quad (3)$$

$$\frac{1}{\rho_i} (\nabla p_i) = \sum_j m_j \left( \frac{p_j}{\rho_j^2} + \frac{p_i}{\rho_j^2} \right) \cdot \nabla_i \hat{w}_{ij} \quad (4)$$

$$\left( \frac{\mu}{\rho} \nabla^2 u \right)_i = \sum_j \frac{4m_j (\mu_i + \mu_j) \vec{r}_{ij} \cdot \nabla_i \hat{w}_{ij}}{(\rho_i + \rho_j)^2 (|\vec{r}_{ij}|^2 + \eta^2)} (\vec{u}_i - \vec{u}_j) \quad (5)$$

Where  $p_{ij}=p_i p_j$ ,  $r_{ij}=r_i-r_j$ ,  $\mu$  is viscosity coefficient and  $\eta$  (which is usually equal to 0.1h) is a small number introduced for keeping the denominator no-zero during the computation.

### 3. ISPH formulation

The ISPH technique is formed by integral interpolation for approximation equations. The extent of function at  $r$  point is explained below (6):

$$f(r_0) = \int_{-\infty}^{\infty} f(r) \delta(r_0 - r) dr \quad (6)$$

Using this integral in numerical analysis is practically impossible. Therefore, Dirac Delta function exchanges with smoothed function and amount of quantify for particle  $i$  is calculated using the following integral (7):

$$f(r_0) = \int_{-\infty}^{\infty} f(r) \delta(r_0 - r) dr \quad (7)$$

This equation is discretized as below (8):

$$f(r_i) = \sum_j \frac{m_j}{\rho_j} f(r_j) \hat{w}(|r_i - r_j|, h) \quad (8)$$

Where  $\Omega$  is support domain,  $m_j$  and  $\rho_j$  are mass and density of particle  $j$ ,  $m_j/\rho_j$  is volume element associated with particle  $j$ ,  $\hat{w}_{ij}$  is smoothing function,  $r$  is position vector,  $h$  is smoothing length which resulted the width of kernel. In this paper,  $h=1.2*dr$  was used, where  $dr$  is initial particle spacing. Smoothing function (9) used in this article (cubic spline) was recommended by [15].

$$w_{ij} = \begin{cases} \frac{10}{7\pi h^2} \left( 1 - \frac{3}{2}q^2 + \frac{3}{4}q^3 \right), & \text{if } 0 \leq q < 1 \\ \frac{10}{28\pi h^2} (2-q)^3, & \text{if } 1 \leq q \leq 2 \\ 0, & \text{otherwise} \end{cases} \quad (9)$$

$q$  is a parameter equal to  $r_{ij}/h$ . Circle radius of central particle ( $kh$ ) will take  $2h$  values. For finding particles in the influence domain of a central particle, if the number of total particles is  $n$ , then  $n^2$  computation is needed that will cause increased calculation load. Therefore, linked list method is used that means searching for 9 squares around the central particle, against using total research of all computational domains [21].

In this method, the computational domain is separated into squares with size  $2h$  and each particle belongs to a square (Figure 1). It is clearly visible that the neighbor particles of the central particle  $i$  are only in 9 squares on every side of the particle interest.

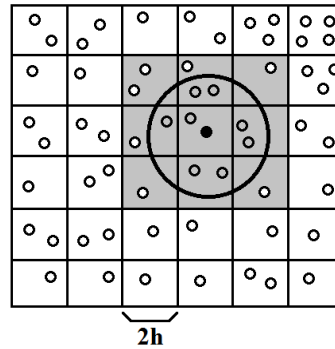


**Figure 1** Dividing of the Computational domain into squares with  $2h$  sizes for finding particles in the influence domain of the central particle.

**4. Solving algorithm**

In this study, the ISPH method with a two-step semi-implicit algorithm has been utilized to solve the governing equations. In the first step, according to the dimensions of the problem and initial distance between particles, fixed particles and mass of all particles is calculated using (10) [12].

$$m_i = \frac{\rho_0}{\sum_j \hat{w}(|r_i - r_j|, h)} \tag{10}$$

Then, mass of all particles can be determined according to (11).

$$\rho_i = \sum_j m_j \hat{w}(|r_i - r_j|, h) \tag{11}$$

In this step, Navier-Stokes equations by ignoring pressure terms (in the absence of incompressible condition) are solved to calculate velocity of particles. Afterwards, velocity  $u_*$  and position particle  $r_*$  are calculated (12-13) [21].

$$u_* = u_t + \Delta u_* \tag{12}$$

$$r_* = r_t + u_* \Delta t \tag{13}$$

$\Delta u_*$  denotes the increment of particle velocity at the prediction step;  $\Delta t$  is the time increment;  $u_t$  and  $r_t$  are the particle velocity and condition at time  $t$ ; and  $u_*$  and  $r_*$  are intermediate particle velocity and condition, respectively. In the next step (correction step), the pressure force, which has been ignored in the last step (prediction step), is used to revise the particle velocity as the following:

$$\vec{\Delta u}^{**} = \frac{-1}{\rho_*} \nabla p_{t+1} \Delta t \tag{14}$$

$$u_{t+1} = u_* + \Delta u_{**} \tag{15}$$

where  $\Delta u_{**}$  stands for the increment of particle velocity at the correction step;  $\rho_*$  is intermediate particle density which was calculated after the prediction step; and  $p_{t+1}$  and  $u_{t+1}$  are the particle pressure and particle velocity at time  $t+1$ . By getting average, the final position of the particle is centered in time as below:

$$r_{t+1} = r_t + \frac{u_{t+1} + u_t}{2} \tag{16}$$

In the above relation,  $r_t$  and  $r_{t+1}$  denote positions of the particle at time  $t$  and  $t+1$ . The Poisson equation is used to calculate the pressure as below:

$$\Delta \left( \frac{1}{\rho_*} \nabla p_{t+1} \right) = \frac{\rho_0 - \rho_*}{\rho_0 \Delta t^2} \quad (17)$$

Where  $\rho_0$  is initial constant density at each of the particles. The advantage of the ISPH method is that large pressure fluctuations can be decreased because of using a strict hydrodynamic formulation.

The pressure in (17) can be solved by either any available direct or iterative solvers. However, the iterative solvers have shown to be more robust in case of great numbers of particles.

## 5. Boundary Conditions (solid walls and free surface)

### 5.1. Solid boundaries

For modelling solid wall, the solid impermeable boundaries are acted by unmoving wall particles. They not only prevent the entrance of inner fluid particles into solid wall but also balance the pressure of them. Because of the pressure balance of fluid particles, Poisson's equation will be solved for these particles. It should be mentioned that two rows of dummy particles out of these walls are placed for ignoring wall particles as free surface particles.

The velocities of wall particles are arranged zero to indicate the unmovable boundary condition.

### 5.2. Free surface

In the ISPH model, the particle density is used to determine the free surface and after that, a zero pressure is given to the free surface particles. Since there is no fluid particle existing in the outside area of the free surface, thereafter the density on the surface particle should drop significantly [17]. For recognizing free surface particles, if the calculated particle density satisfies the following condition, the particle is recognized as a surface particle [5].

$$\rho_* < \beta \times \rho_0 \quad (18)$$

In (18),  $\beta$  is free surface parameter and  $0.8 < \beta < 0.99$ . In this paper,  $\beta = 0.97$  was used.

## 6. Modelling of free surface flows with ISPH model

Three free surface problems have been considered to show the model's capabilities and to investigate its accuracy. Two dam-break sudden and gradual flood wave problems and the solitary wave in open-channel on a stiff bed are used to illustrate the model's capacity to calculate the free-surface position and the distort of the water surface. The numerical results have been contrasted to experimental measurements and analytical solution.

### 6.1. Modelling of sudden dam-break flood wave Flow against an isolated obstacle

This experiment was done by the first author in the Civil Engineering Laboratory of the Islamic Azad University (Sirjan Branch, Iran). The flume dimensions are indicated in Figure 2. Because of the immediate Removability of the gate from the water column, it could be considered as a sudden dam-break. In addition to recent computations, water density was considered 1000 kg/m<sup>3</sup> and water dynamics viscosity was about 0.001 N.s/m<sup>3</sup>. For performing this simulation, 3229 particles with initial between-particle distance of 0.006 m were used. Comparison of experimental results and the results of numerical modelling the dam-break flow in contrast to a rigid obstacle (as shown in Figure 3) shows the position of particles and free-surface shape, and pressure distribution after a 0.1, 0.3, 0.5 and 0.7 s simulation. Figure 4 shows the pressure distribution resulted from the numerical model for simulation of 0.3 and 0.7 s.

It may be seen that the predicted free-surface shape has an acceptable adaptation of the experimental observations. For better understanding and more accurate analysis of results, normalized diagram of time in comparison to position proceeding of wave front of numerical model with the distance of 0.006 m between particles and experimental model is given in Figure 5.

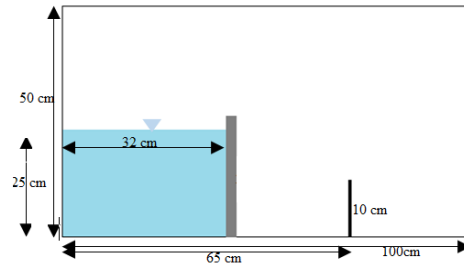


**Figure 2** Initial geometry of sudden collapse of free water column (dam-break) in contrast to a rigid obstacle (dam-break) with initial height of 25 cm.

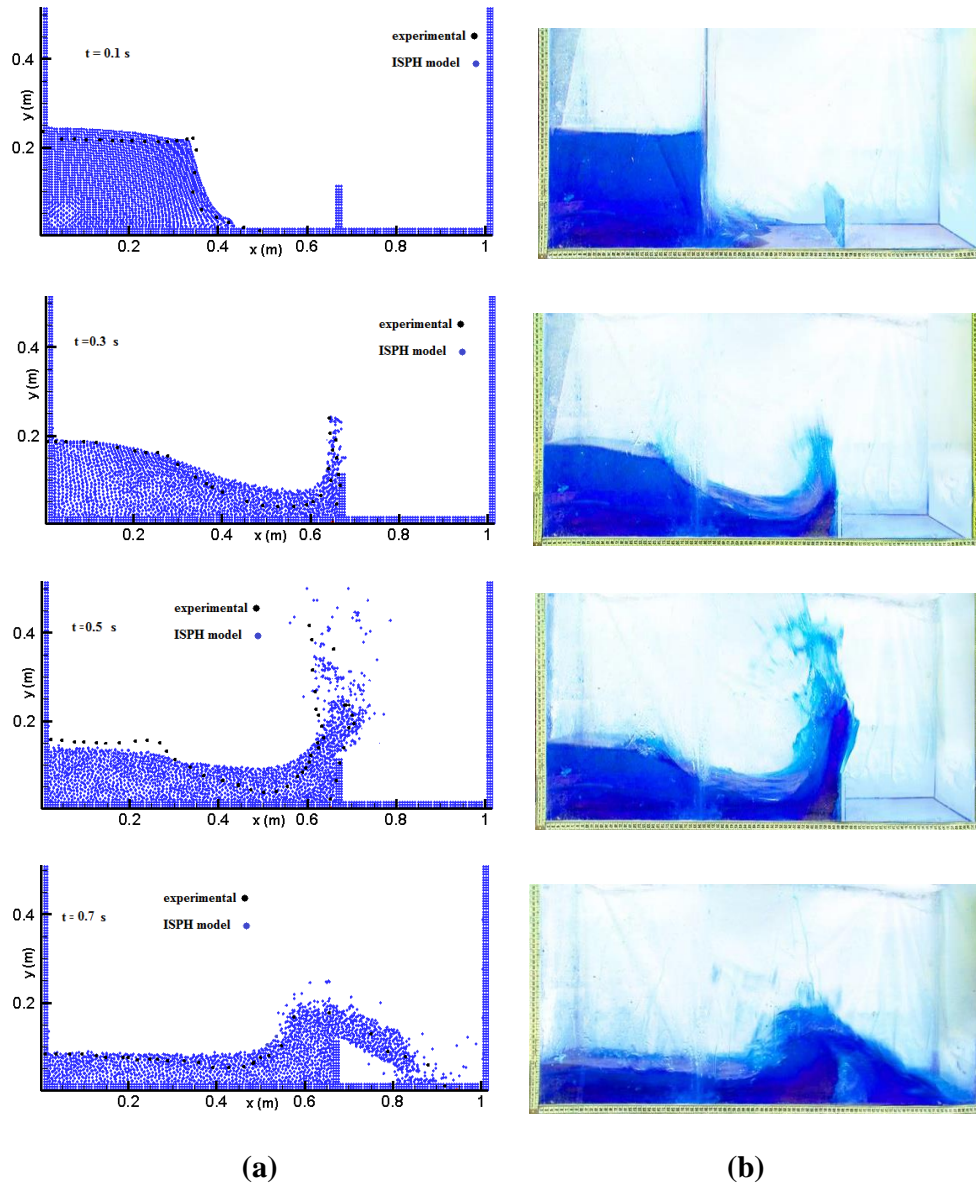


**Figure 3** Comparison of (a) numerical results and (b) experimental observations; the observed digitized free-surface position is denoted by the black circle in (a).

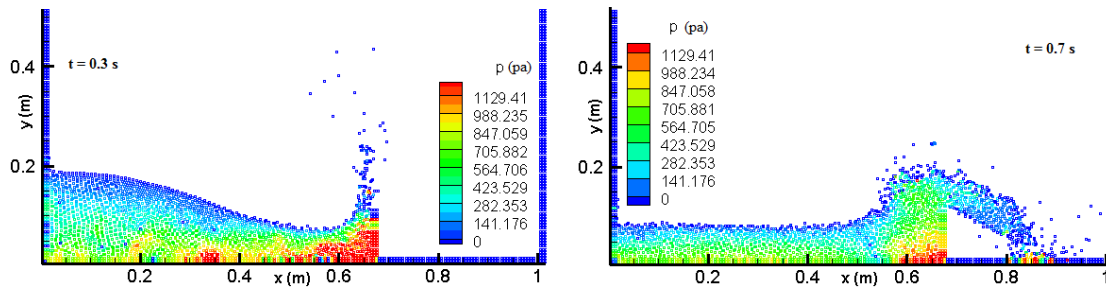


**Figure 4** calculated Pressure contours by the ISPH model in 0.3 s and 0.7 s for the dam-break flow in contrast to a rigid obstacle test case.

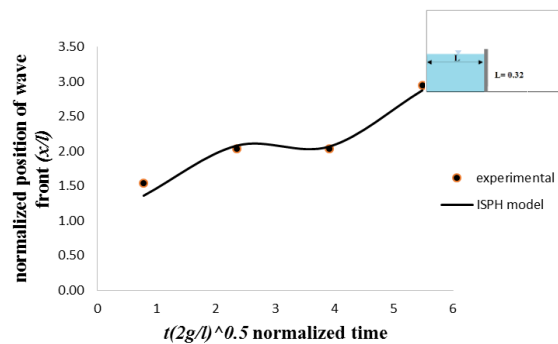


**Figure 5** Comparison of numerical and experimental normalized graph of the location of the wave front for the dam-break wave flow against a rigid obstacle test case.

**TABLE 1.** Evaluation of the ISPH numerical model via relative error statistic for the dam-break flood wave against an isolated obstacle test case.

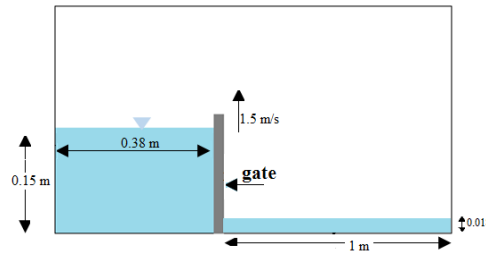
Time(s)	Relative error of wave height %	Relative error of wave position %
0.1	7.9	11.9
0.3	5.73	-2.18
0.5	13.01	-1.59
0.7	10.18	2.5
Mean %	9.15	3.29

Results were analyzed considering the position of proceeding wave front and flow height against time. For evaluating the numerical method, mean relative error was used (Table 1).

Table 1 shows that mean relative error in the computation of the position of the wave front was 3.29%. Furthermore, mean relative error in computing flow height was less than 9.15%. Comparison of numerical and experimental results shows good accuracy in flow simulation of dam-break test case with a downstream obstacle.

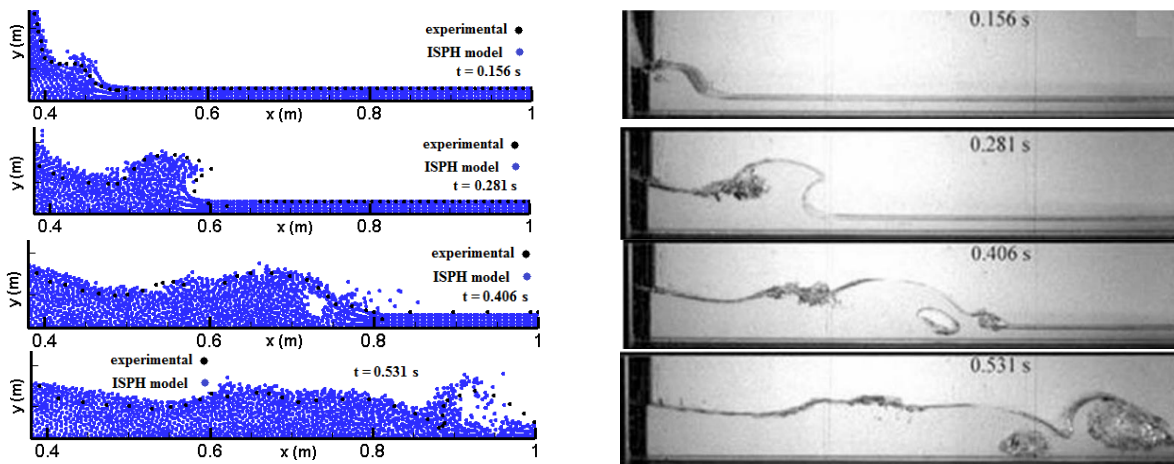
## 6.2. Modelling gradually collapse of Water column (dam break) on a wet bed

In this test case, the experimental observations were taken from [10]. The experimental setup is mentioned in Figure 6. In the initial time, water column with a depth of 0.15 m is blocked by a gate. The initial downstream water depth is set as 0.018 m. The flood wave propagates as the gate opens completely from above with a constant speed of 1.5 m/s. As for the numerical simulation, in total, 5930 particles with an initial distance of 0.004 m were used.



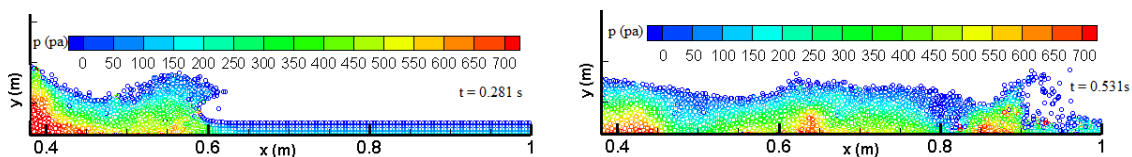
**Figure 6** Initial geometry of gradually collapse of free water column (dam-break) with initial height of 0.15 m and gate velocity of 1.5 m/s.

Figure 7 compares the numerically calculated water surface with the digitized experimental water surface in four different time steps. As may be seen from Figure 7, there is some discrepancy between the numerical consequences and the experimental observation in the initial stage of the free-surface change. However, it should be noted that the mushroom-shaped water surface observed in the numerical results has also been reported by [14], [3] and [9]. In general, the calculated free water-surface features are in acceptable agreement with the experimental observations.



**Figure 7** Comparison of (above) numerical results and (below) experimental observations (reprinted from [20]); the observed digitized free-surface position is denoted by the black circle in (a).

Figure 8 shows the position of particles, free-surface shape, and pressure distribution after a 0.281 and 0.531 s simulation. Normalized diagram of time in comparison to position proceeding of wave front of numerical model with the distance of 0.004 m between particles and experimental model is given in Figure 9.



**Figure 8** Pressure contours calculated by the ISPH model in 0.281 s and 0.531 s after the first time for gradually collapse of the water column test case.

Summary of the numerical model evaluation using relative error statistic criterion is shown in Table 2. Table 2 shows that mean relative error in the computation of the position of the wave front was 1.73%. Furthermore, mean relative error in computing flow height was less than 8.3%. Comparing the numerical results and experimental observations, confirms the ability of the developed numerical model in flow simulation of gradual flood wave over wet bed.



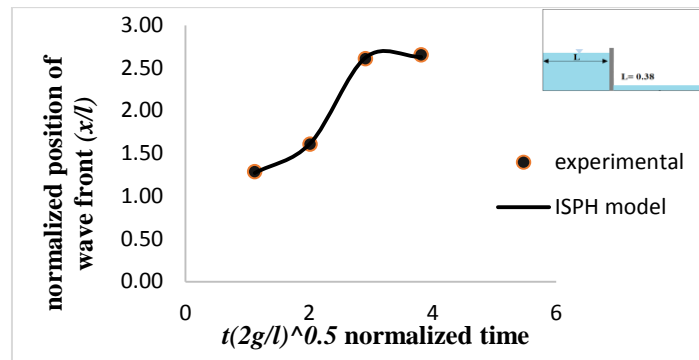


**Figure 9** Comparison of numerical and experimental normalized diagram of the position of the wave front for gradually collapse of water column case.

**TABLE 2** Evaluation of the ISPH numerical model via relative error statistic of the position of the wave front for gradually collapse of water column test case.

Time (s)	Relative error of Wave height %	Relative error of Wave position %
0.156	7.4	2.12
0.281	8.2	1.6
0.406	7.8	1.23
0.531	10	2.0
Mean %	8.3	1.73

### 6.3. Modeling of solitary wave

In this part, the accuracy of ISPH flow model is assessed by analogizing the numerical and theoretical wave heights of a solitary wave propagating on an isolated bed. Considering the following relation (which is derived from the Boussinesq equation), the initial wave situation was arranged by identifying the particles near the computational entrance regarding an analytical solitary wave profile and velocity derived from the Boussinesq equation [21].

$$\eta(x,t) = a \operatorname{sech}^2 \left[ \sqrt{\frac{3a}{4d^3}} (x - ct) \right] \quad (19)$$

where  $\eta$  = water surface elevation,  $a$  = wave amplitude,  $d$  = water depth and  $c = \sqrt{g(d+a)}$  is the solitary wave celerity. The horizontal velocity under the wave profile is calculated by (20)

$$u = \eta \sqrt{\frac{g}{d}} \quad (20)$$

In this study, a solitary wave with the wave amplitude  $a=0.06$  m is considered. The water depth is 0.2 m and the initial particle spacing is 0.01 m. The first situation was arranged by identifying the particles near the computational entrance with the wave profile of Eq. (19), zero vertical velocity and horizontal velocity of Eq. (20). As for the numerical computation, the 5200 particles were placed on a regular grid with square cells, in a way that those that were above the profile were eliminated. This condition leads to a slightly rough initial profile such that the fluid rapidly adjusts to the solitary wave profile. Figure 10 indicates the comparisons of the modeled wave profiles and the analytical answers at various times.

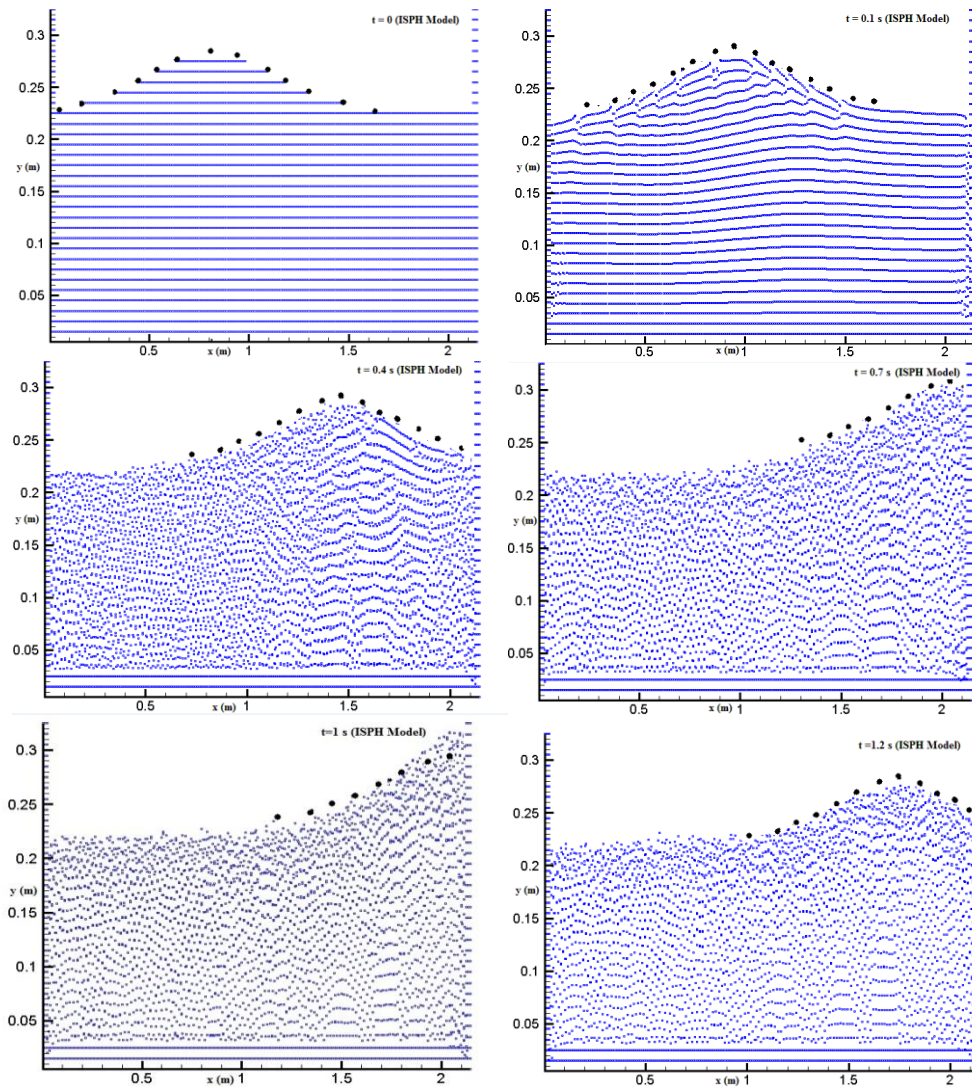


**Figure 10** Comparisons of modeled (the blue points) and analytical (the black points) solitary wave profiles at 0.1, 0.4, 0.7, 1 and 1.2 s.

Results of simulations are indicated acceptable agreement between the numerical and the analytical calculations. However, according to the results at  $t=1$  s (where the wave deals the right wall) a reduction in the accuracy of the numerical model can be observed. This problem is due to an error which is usually occurs in the numerical solution of Poisson's equation.

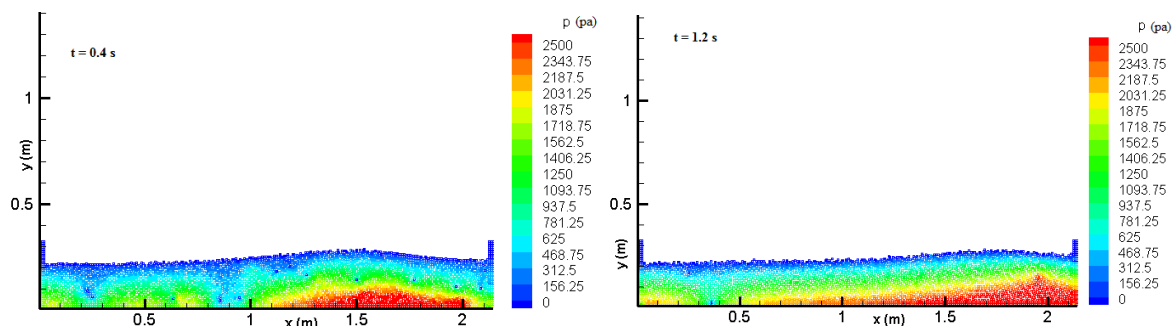


**Figure 11** Calculated pressure contours by the ISPH numerical model in 0.4 s and 1.2 s.

In Figure 11, the pressure contours at the time of 0.4 s and 1.2 s are shown. As may be observed the pressure contours are almost regular. At the time of 0.4 s, the pressure at the peak of wave approximately equals to the hydrostatic pressure measured at this point ( $\approx 2900$  pa). Figures 12 and 13 respectively indicate the normalized diagram of time in comparison to position of solitary wave and

the normalized diagram of time in comparison to solitary wave height.

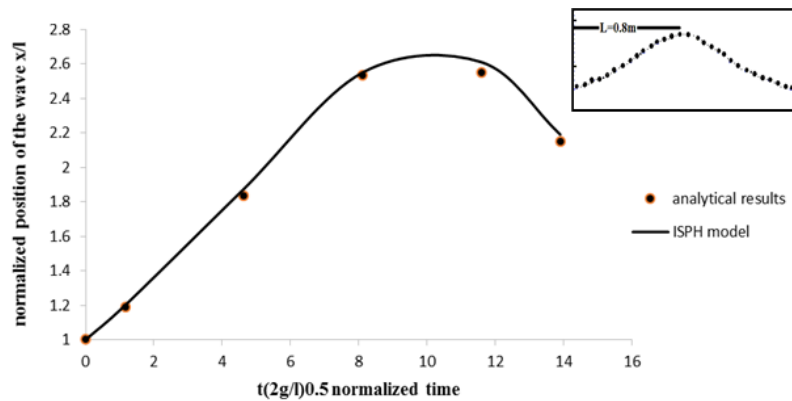


**Figure 12** Normalized diagram of time compared to condition of the solitary wave front and its comparison with the analytical results for the solitary wave test case.

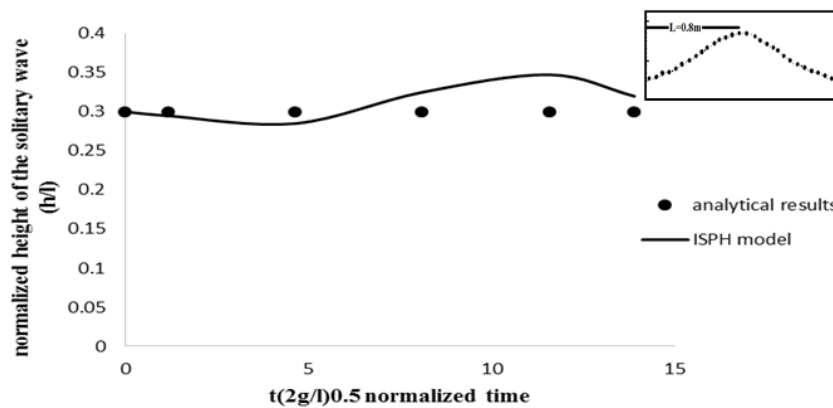


**Figure 13** Normalized diagram of time compared to height of the solitary wave and its comparison with the analytical results.

The comparison for the wave height between the calculated results and observation in terms of relative error are presented in Table 3.

**TABLE 3** Evaluation of the ISPH numerical model via relative error statistic of the position of the wave front for the solitary wave test case.

Time(s)	Relative error of wave height %	Relative error of wave front position %
1	1.6	-1.05
0.4	3.3	-2.04
0.7	-5	-0.69
1	-11	-2.45
1.2	-6.6	-1.9
Mean %	5.5	1.62

## 7. Conclusion

The purpose of present study was to provide insight into mesh-free ISPH simulation of free surface hydraulics problems and challenge the capabilities of this method in the field of computational fluid dynamics.

The ISPH model was applied for flow simulation of three test cases of dam-break flood wave, gradual collapse of water column and solitary wave. Governing equations on wave flows were solved using ISPH discrete method with two-step fractional algorithm. The initial distance of 0.006 m for the dam-break test, 0.004 m for gradual water collapse and 0.01 m for solitary wave case were considered

between particles.

In order to assess the ability of the numerical method, mean relative error was used. The mean relative error in the computation of the position of the wave front of the dam-break and water column collapse were below 4%. Furthermore, mean relative error in computing flow height of these two cases were below 10%. Moreover, the mean relative error in the computation of the height of the solitary wave was 5.5% and mean relative error of Wave position was equal to 1.62 %. These outcomes demonstrated the ability of the advanced model to deal with a realistic free-surface problem even when large deformations exist in the free surface.

## References

1. A. Shakibaenia and Y. Jin, MPS-Based Mesh-Free Particle Method for Modeling Open-Channel Flows, *Hydraul. Eng J.*, 137(2011), pp. 1375–1384.
2. A. Colagrossi and M. Landrini, Numerical simulation of interfacial flows by smoothed particle hydrodynamics, *Comput. Phys J.*, 191(2003), pp. 448-475.
3. A.J.C. Crespo, M. Gómez-Gesteira and R.A. Dalrymple, Modeling dam break behavior over a wet bed by a SPH technique, *Waterw. Port Coastal Ocean Eng J.*, 134(2008), pp. 313–320.
4. B. Ataie-Ashtiani and G. Shobeyri, Numerical simulation of landslide impulsive waves by incompressible smoothed particle hydrodynamics, *Int. J. Numer. Methods Fluids.*, 56 (2008), pp. 209-232.
5. B. Ataie-Ashtiani, G. Shobeyri and L. Farhadi, Modified incompressible SPH method for simulating free surface problems, *Fluid Dyn. Res J.*, 40(2008), pp. 637-661.
6. C. Altomare, A.J.C. Crespo, J.M. Domínguez, M. Gómez-Gesteira, T. Suzuki and T. Verwaest, Applicability of Smoothed Particle Hydrodynamics for estimation of sea wave impact on coastal structures, *Coastal Eng J.*, 96(2015), pp. 1-12.
7. E. Džebo, D. Žagar, M. Krzyk, M. Četina and G. Petkovšek, Different ways of defining wall shear in smoothed particle hydrodynamics simulations of a dam-break wave, *Hydraulic Research J.*, 52(2014), pp. 453-464.
8. E. Fontaine, M. Landrini and M. Tulin, Breaking: Splashing and ploughing phases, *Int. Workshop on Waterwaves and Floating Bodies J.*, 4(2000), pp. 34 –38.
9. E.S. Lee, C. Moulinec, R. Xu, D. Violeau, D. Laurence and P. Stansby, Comparisons of weakly compressible and truly incompressible algorithms for the SPH mesh free particle method, *Comput. Phys J.*, 227(2008), pp. 8417–8436.
10. I. Janosi M, D. Jan, K.G. Szabo and T. Tel, Turbulent drag reduction in dam-break flows, *Exp. Fluids J.*, 37(2004), pp. 219–229.
11. J.J. Monaghan, SPH without a tensile instability, *Comput. Phys J.*, 159(2000), pp. 290-311.
12. J. Monaghan and A. Kos, Solitary waves on a Cretan beach, *Waterw. Port Coastal Ocean Eng J.*, 125(1999), pp. 145-155.
13. P. Jonsson, P. Jonsén, P. Andreasson, TS. Lundström, J. Gunnar and I. Hellström, Modelling Dam Break Evolution over a Wet Bed with Smoothed Particle Hydrodynamics: A Parameter Study, *Engineering J.*, 7(2015), pp. 248-260.
14. P.K. Stansby, A. Chegini and T.C.D. Barnes, The initial stages of dam-break flow, *Fluid Mech J.*, 374(1998), pp. 407-424.
15. R.A. Dalrymple, O. Knio, Dn.T. Cox, M. Gesteira and S. Zou, Using a Lagrangian particle method for deck overtopping, *Proc., Waves J.*, (2002), pp. 1082–1091.
16. R. Gingold and J.J. Monaghan, Smoothed particle hydrodynamics: theory and application to non-spherical stars, *Mon. Not. R. Astron. Soc J.*, 181(1977), pp. 375-389.
17. R. Xu, P. Stansby and D. Laurence, Accuracy and stability in incompressible SPH (ISPH) based on the projection method and a new approach, *Comput. Phys J.*, 228(2009), pp. 6703-6725.
18. S. Lind, R. Xu, P.K. Stansby and B.D. Rogers, Incompressible smoothed particle hydrodynamics for free-surface flows: A generalised diffusion-based algorithm for stability and validations for impulsive flows and propagating waves, *Comput. Phys J.*, 231(2012), pp. 1499–1523.

19. S. Lind, P.K. Stansby and B.D. Rogers and P.M. Lloyd, Numerical predictions of water–air wave slam using incompressible–compressible smoothed particle hydrodynamics, *Appl. Ocean Res J.*, 49(2015), pp. 57-71.
20. S. Shao and E.Y. Lo, Incompressible SPH method for simulating Newtonian and non-Newtonian flows with a free surface, *Adv. Water Resour J.*, 26(2003), pp. 787-800.
21. S. Shao, Incompressible SPH flow model for wave interactions with porous media, *Coastal Eng J.*, 57(2010), pp. 304-316.